INSTITUTE OF FLUID-FLOW MACHINERY
POLISH ACADEMY OF SCIENCES

TRANSACTIONS OF THE INSTITUTE OF FLUID-FLOW MACHINERY

108

WYDAWNICTWO IMP PAN

GDAŃSK 2001

TRANSACTIONS OF THE INSTITUTE OF FLUID-FLOW MACHINERY Appears since 1960

Aims and Scope

Transactions of the Institute of Fluid-Flow Machinery have primarily been established to publish papers from four disciplines represented at the Institute of Fluid-Flow Machinery of Polish Academy of Sciences, such as:

- Liquid flows in hydraulic machinery including exploitation problems,
- Gas and liquid flows with heat transport, particularly two-phase flows,
- Various aspects of development of plasma and laser engineering,
- Solid mechanics, machine mechanics including exploitation problems.

The periodical, where originally were published papers describing the research conducted at the Institute, has now appeared to be the place for publication of works by authors both from Poland and abroad. A traditional scope of topics has been preserved.

Only original and written in English works are published, which represent both theoretical and applied sciences. All papers are reviewed by two independent referees.

EDITORIAL AND PUBLISHING OFFICE

IFFM Publishers (Wydawnictwo IMP), Institute of Fluid Flow Machinery, Fiszera 14, 80-952 Gdańsk, Poland, Tel.: +48(58)3411271 ext. 141, Fax: +48(58)3416144, E-mail: esli@imp.gda.pl

Financial support of publication of this journal is provided by the State Committee for Scientific Research, Warsaw, Poland

Terms of subscription

Subscription order and payment should be directly sent to the Publishing Office

Warunki prenumeraty w Polsce

Wydawnictwo ukazuje się przeciętnie dwa lub trzy razy w roku. Cena numeru wynosi 20,- zł + 5,- zł koszty wysyłki. Zamówienia z określeniem okresu prenumeraty, nazwiskiem i adresem odbiorcy należy kierować bezpośrednio do Wydawcy (Wydawnictwo IMP, Instytut Maszyn Przepływowych PAN, ul. Gen. Fiszera 14, 80-952 Gdańsk). Osiągalne są również wydania poprzednie. Prenumerata jest również realizowana przez jednostki kolportażowe RUCH S.A. właściwe dla miejsca zamieszkania lub siedziby prenumeratora. W takim przypadku dostawa następuje w uzgodniony sposób.

ISSN 0079-3205

TRANSACTIONS OF THE INSTITUTE OF FLUID-FLOW MACHINERY
No. 108, 2001, 73-94

VITALIJ GNESIN[1], ROMUALD RZĄDKOWSKI[2]

Aeroelastic behaviour of the last stage steam turbine blades. Part II. Coupled fluid-structure oscillations

This paper presents the partial integrated method which has been employed for aeroelasticity predictions of the long steam turbine blades. The approach is based on the solution of the coupled fluid – structure problem in which the aerodynamic and structural dynamic equations are integrated simultaneously in time, thus providing the correct formulation of a problem. The ideal gas flow around the blade row is described by the unsteady 3D Euler equations in conservative form, which are integrated by using the explicit monotonous second-order accurate Godunov-Kolgan, finite volume scheme and moving grids. In the structural analysis the modal approach is used. The natural frequencies and modal shapes of the blade were calculated by using 3D finite element model. The coupled fluid-structure oscillations were shown for 5 modes shapes separately and with taking into account the interaction of five natural modes.

1. Introduction

Modern turbomachines operate under very complex flow regimes where a mixture of subsonic, transonic and supersonic regions coexist.

Recent times the new approaches based on the simultaneous integration in time of the equations of motion for the structure and the fluid are developed (Marshal and Imregun [1], Bakhle et al. [2], He [3]; Moyround et al. [4], Rządkowski et al. [5], He and Ning [6], Bendiksen [7], Gnesin et el. [8-9], Carstens and Belz [10], Gnesin et al. [11]). These approaches are very attractive due to the correct formulation of a coupled problem, as the interblade phase angle at which the stability (instability) would occur is a part of solution.

In the present study the simultaneous time integration method has been described to calculate the aeroelastic behaviour for a three-dimensional oscillating long steam turbine blade in the transonic gas flow. The coupled fluid-structure

[1]Institute of Problems in Machinery, Ukrainian National Academy of Sciences, 2/10 Pozharsky st., Kharkov 310046, Ukraine

[2]Institute of Fluid Flow Machinery, Polish Academy of Sciences, Fiszera 14, 80-952 Gdańsk, Poland

oscillations were shown for 5 modes shapes separately and with taking into account the interaction of five natural modes.

2. Aerodynamic model

In the present work considered is the 3D transonic flow of an ideal gas through a space multipassage blade row. In general case the flow is assumed to be aperiodic function from blade to blade (in pitchwise direction), so the calculated domain includes all blades of the whole assembly.

The ideal gas flow around blade row is described by the unsteady 3D Euler equations in conservative form, which are integrated by using the explicit monotonous second-order accurate Godunov-Kolgan, finite volume scheme and moving grids.

The aerodynamic model was presented in details by Gnesin & Rządkowski [12].

3. Structural model

The structural model is based on a linear model, the mode shapes and natural frequencies being obtained via standard FE analysis techniques. The mode shapes are interpolated from the structure mesh onto aerodynamic mesh.

The structural part of the aerodynamic equations of motion can be uncoupled by using the mode shape matrix and the modal superposition method (see Rządkowski [14], Gnesin and Rządkowski [12]).

Boundary conditions from the structural and aerodynamic domains are exchanged at each step and the aeroelastic mesh is moved to follow the structural motion.

4. Numerical results

The numerical calculations have been carried out for the long steam turbine cascade. The important properties of the blade disc are as given below: the disk inner radius: $r_o = 0.27$ m, the bladed-disk junction radius: $R = 0.667$ m, the blade length: $L = 0.765$ m. All geometrical parameters of the blade are presented in Rządkowski [14].

In paper [16] the individual stability of each mode in turn for a harmonic oscillation with the assumed interblade phase angle is shown.

In this paper the numerical results of coupled oscillations for each of natural modes at the IBPA values corresponding to the minimal values of aerodamping coefficient are presented and next the interaction between five modes is considered. The excitation frequencies were chosen close to the natural frequencies.

4.1. The coupled oscillations of the blade row when considering one of five natural modes separately

The aeroelastic response of the blade row vibrating according to the 1^{st} mode, the excitation frequency of 50 Hz and IBPA equal to -90 deg. is presented in Fig.

1. In Fig. 2 the aerodamping coefficient distribution over the blade length at the harmonic oscillations has been shown. The transfer of energy from the flow to the blade (flutter condition) appeared from the root to 4/5 of the blade length and the dissipation of blade energy took place in the tip blade region. The averaged aerodamping coefficient over the blade length takes the positive value ($D = 0.02$), that corresponds to the stability of the blade oscillation.

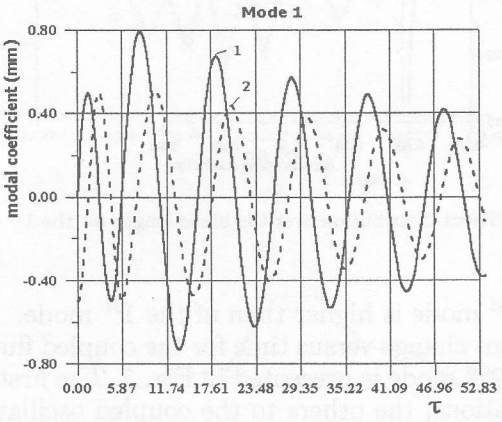

Fig. 1. The coupled oscillations according to the 1^{st} mode for two adjacent blades, IBPA= -90 deg, $\delta = 0.155$, $t = \tau/316$ s.

All calculations were run from the very beginning for harmonic oscillations. After some time, at the moment named as the started regime, there began the coupled vibrations (the coupled fluid-structure interaction). Figure 1 illustrates the response of two adjacent blades. The harmonic oscillation continued through one period then the coupled vibration began. It can clearly be observed that the amplitude of oscillations according to the 1^{st} mode decay.

The logarithmic decrement (loddec), is defined as

$$\delta = \frac{1}{n} \ln \frac{A_1}{A_n} ,$$

where n is the number of cycles; A_1 and A_n are amplitudes of the first cycle and n-th cycle of blade oscillation.

In this case the logarithmic decrement is equal to $\delta = 0.155$.

The work coefficient for each of blades (four passages in this case) is shown in Fig. 3a and for the blade row as a whole is presented in Fig. 3b. The monotonous convergence of the work coefficient to zero demonstrates the dissipation of the vibrating blades energy to the flow field.

The aeroelastic response of the blade row vibrating according to the 2^{nd} mode and the excitation frequency of 100 Hz and IBPA equal to 0 deg was calculated.

The aerodamping coefficient distribution over the blade length at the harmonic oscillations is presented in Fig. 4. The averaged aerodamping coefficient for harmonic oscillations according to the 2^{nd} mode is positive and equal to 0.09.

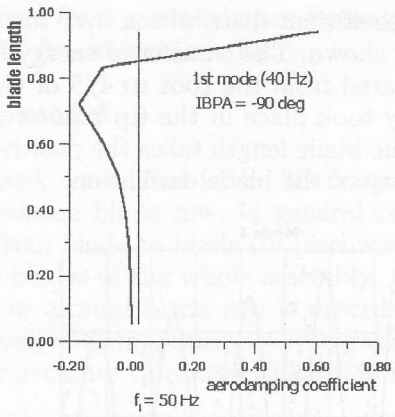

Fig. 2. The aerodamping coefficient distribution over the blade length for the 1^{st} mode, IBPA= -90 deg.

The stability of the 2^{nd} mode is higher than of the 1^{st} mode.

The modal coefficient change versus time for the coupled fluid-structure vibrations according to the 2^{nd} mode is presented in Fig. 5. The first cycle corresponds to the harmonic oscillations, the others to the coupled oscillations. The coupled vibrations decay. The logarithmic decrement for this mode of vibration is equal to $\delta = 0.195$. The work coefficient for the blade row as a whole is presented in Fig. 6. The monotonous convergence of the work coefficient to zero demonstrates the dissipation of the vibrating blades energy to the flow field. In Fig. 7 the phase trajectory for the oscillations according to the 2^{nd} mode is presented. The bold ellipse corresponds to the harmonic oscillations, and the spiral corresponds to aerodamping.

The aeroelastic response of blade row vibrating according to the 3^{rd} mode, the excitation frequency of 200 Hz and IBPA equal to 90 deg has been calculated.

The averaged aerodamping coefficient for harmonic oscillations according to the 3^{rd} mode is negative and equal to -0.25 (see Fig. 8).

The modal coefficient versus time for the coupled fluid-structure vibrations according to the 3^{rd} mode is presented in Fig. 9. The first cycle corresponds to the harmonic oscillations, the others to the coupled oscillations. The coupled vibrations decay. The logarithmic decrement corresponding to this mode is equal to $\delta = 0.2$.

In Fig. 10 the phase trajectory for the oscillations according to the 2^{nd} mode is presented. The bold ellipse corresponds to the harmonic oscillations, and the spiral corresponds to aerodamping.

The work coefficient for each of blades (four passages in this case) is shown in Fig. 11 and for the blade row as a whole is presented in Fig. 12. The monotonous convergence of the work coefficient to zero demonstrates the dissipation of the vibrating blades energy to the flow field.

However, the flutter conditions appeared in the harmonic oscillations, the blade response in the coupled vibration decreases. This fact can be explained in

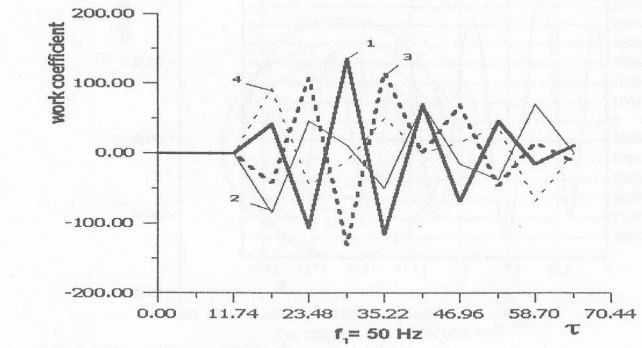

a)

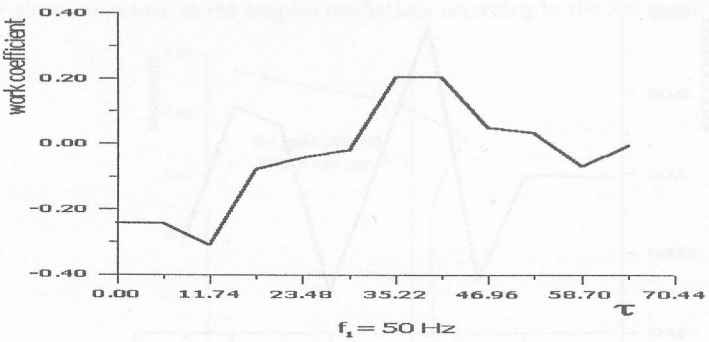

b)

Fig. 3. The work coefficient change at the coupled oscillations according to the 1^{st} mode,IBPA= -90 deg, $t = \tau/316$ s.

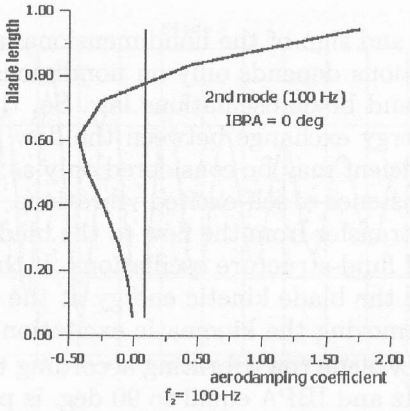

Fig. 4. The aerodamping coefficient distribution over the blade length for the 2^{nd} mode, IBPA= 0 deg.

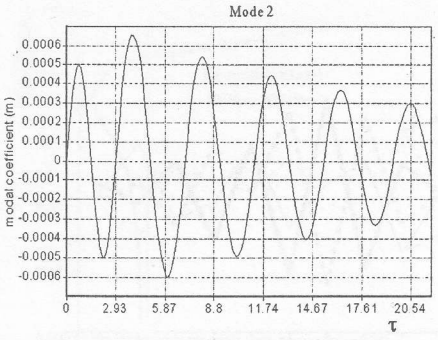

Fig. 5. The coupled oscillations according to the 2^{nd} mode and IBPA= 0 deg, $\delta = 0.195$, $t = \tau/316$ s.

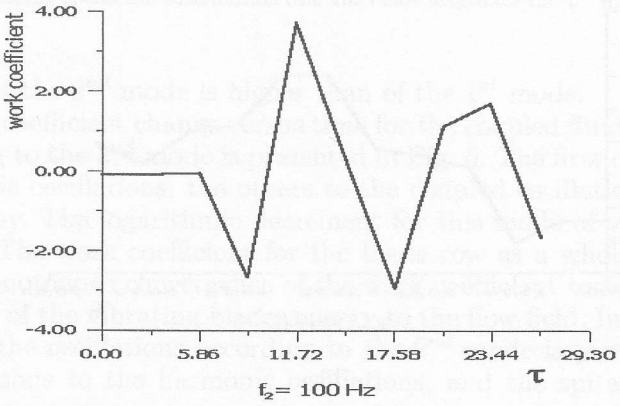

Fig. 6. The work coefficient change at the coupled oscillations according to the 2^{nd} mode and IBPA= 0 deg, $t = \tau/316$ s.

the following way. The value and sign of the nondimensional aerodamping coefficient at the harmonic oscillations depends only on nondimensional aerodynamic parameters of the flow field and blade oscillations law. So, the aerodamping coefficient characterizes the energy exchange between the flow and the blade. The sign of the aerodynamic coefficient may be considered only as a necessary but not sufficient condition for the existence of self-excited vibrations. The blade response depends on the energy value transfer from the flow to the blade, and on the blade kinetic energy at the coupled fluid-structure oscillations. If the value of transferring energy is much less than the blade kinetic energy at the coupled vibrations, the blade oscillations after removing the kinematic excitation are damped.

The aeroelastic response of blade row vibrating according to the 4^{th} mode, the excitation frequency of 220 Hz and IBPA equal to 90 deg. is presented in Fig. 14. The averaged aerodamping coefficient is equal to -0.1 (see Fig. 13).

In Fig. 15 the phase trajectory for the oscillations according to the 2^{nd} mode is presented. The bold ellipse corresponds to the harmonic oscillations, and the

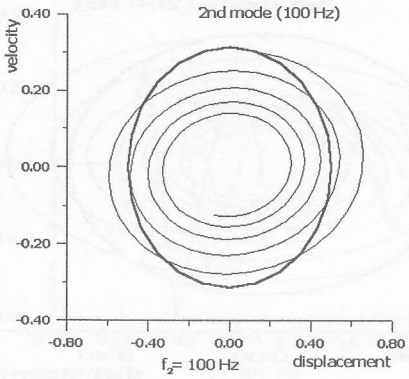

Fig. 7. The phase trajectory at the coupled oscillations according to the 2^{nd} mode and IBPA = 0 deg.

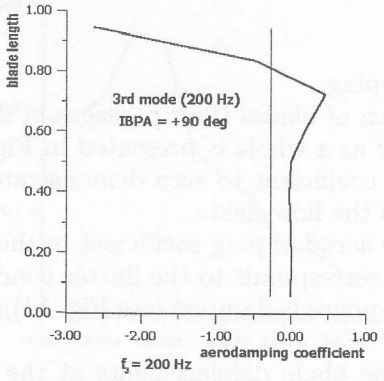

Fig. 8. The aerodamping coefficient distribution over the blade length for the 3^{rd} mode and IBPA= +90 deg.

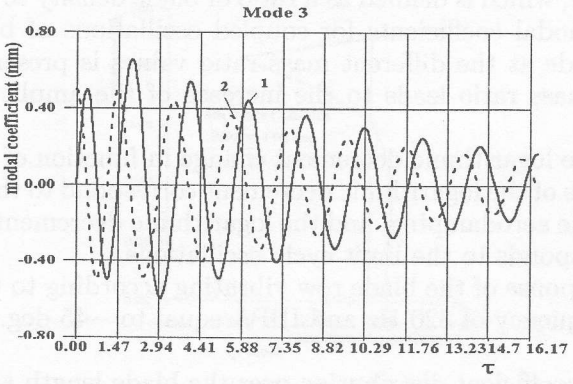

Fig. 9. The coupled oscillations according to the 3^{rd} mode, IBPA= +90 deg, $\delta = 0.2$.

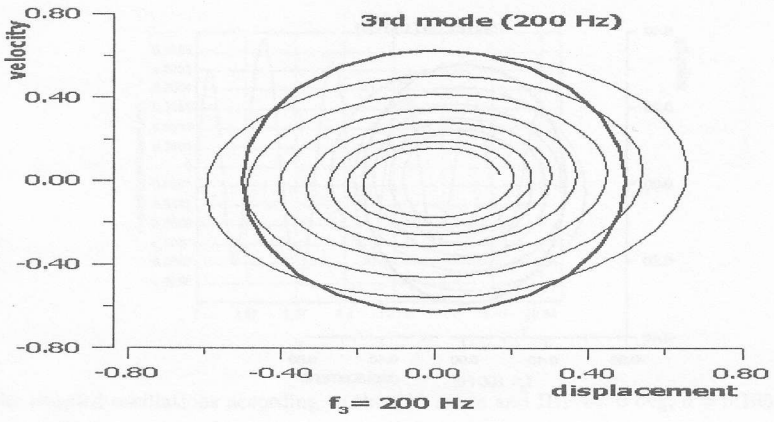

Fig. 10. The phase trajectory at the coupled oscillations according to the 3^{rd} mode and IBPA = +90 deg.

spiral corresponds to aerodamping.

The work coefficient for each of blades (four passages in this case) is shown in Fig. 16a and for the blade row as a whole is presented in Fig. 16b. The monotonous convergence of the work coefficient to zero demonstrates the dissipation of the vibrating blades energy to the flow field.

As in the previous case the aerodamping coefficient in the harmonic vibration takes the negative value, that corresponds to the flutter condition, but in the coupled oscillations the blade response is damped (see Fig. 14) with the logarithmic decrement equal to 0.195.

It should be noted that the blade displacements at the coupled oscillations depend not only on IBPA and excitation frequency, but also on such parameters as the mass flow rate and mass of the blade. Let us input into consideration the mass ratio coefficient μ, which is defined as a ratio of blade density to flow density.

The change of modal coefficients for coupled oscillations of blade row according to the 4^{th} mode at the different mass ratio values is presented in Figs. 17. The decrease of mass ratio leads to the increase of the amplitude of blade oscillation.

Figure 18 shows the logarithmic decrement change in function of the mass ratio. The negative values of the logarithmic decrement correspond to the self-excitation, the positive value to the aerodamping, and the logarithmic decrement value which is equal to zero, corresponds to the limit cycle oscillations.

The aeroelastic response of the blade row vibrating according to the 5^{th} mode and the excitation frequency of 320 Hz and IBPA equal to -45 deg. is presented in Fig. 20.

The aerodamping coefficient distribution over the blade length at the harmonic oscillations is presented in Fig. 19. The averaged aerodamping coefficient for harmonic oscillations according to the 2^{nd} mode is positive and equal to 0.3.

The work coefficient for each of blades (four passages in this case) is shown in

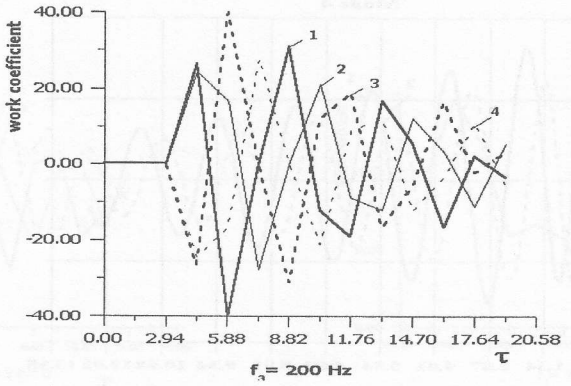

Fig. 11. The phase trajectory at the coupled oscillations according to the 2^{nd} mode and IBPA = 0 deg.

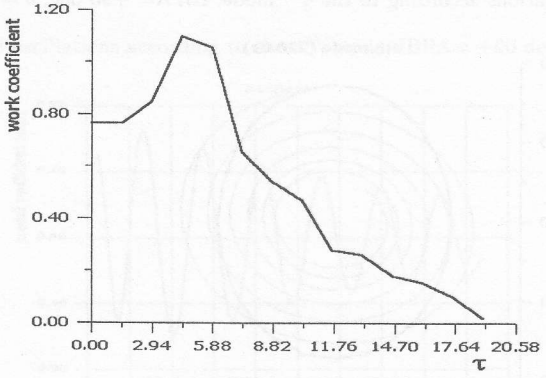

Fig. 12. The aerodamping coefficient distribution over the blade length for the 3^{rd} mode and IBPA= +90 deg.

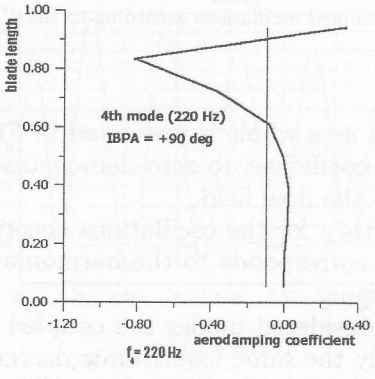

Fig. 13. The coupled oscillations according to the 3^{rd} mode, IBPA= +90 deg, $\delta = 0.2$.

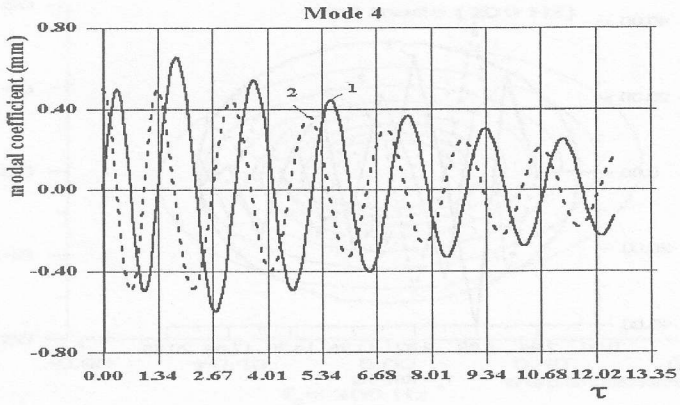

Fig. 14. The coupled oscillations according to the 4^{th} mode, IBPA= +90 deg, $\delta = 0.195$, $t = \tau/316$ s.

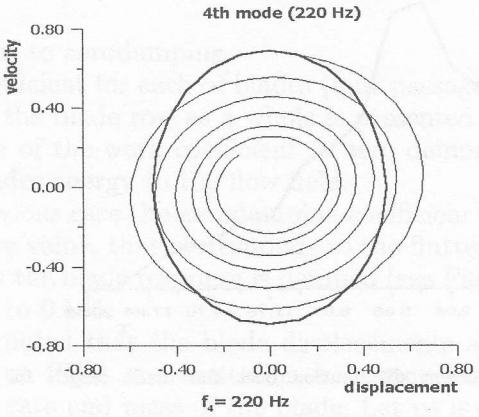

Fig. 15. The phase trajectory at the coupled oscillations according to the 4^{th} mode, IBPA= +90 deg.

Fig. 21a and for the blade row as a whole is presented in Fig. 21b. The monotonous convergence of the work coefficient to zero demonstrates the dissipation of the vibrating blades energy to the flow field.

In Fig. 22 the phase trajectory for the oscillations according to the 5^{th} mode is presented. The bold ellipse corresponds to the harmonic oscillations, and the spiral corresponds to aerodamping.

It is found that for each considered modes the coupled damping oscillations are realised with approximately the same logarithmic decrement ($\delta \approx 0.195$) but with different frequencies of coupled vibration. Generally, the frequency of the coupled vibration decreases from 40 to 50% in comparison to the excitation harmonic frequency (see Figs. 2, 5, 9, 14, 20). So the damping time is inversely proportional to the excitation frequency of oscillations.

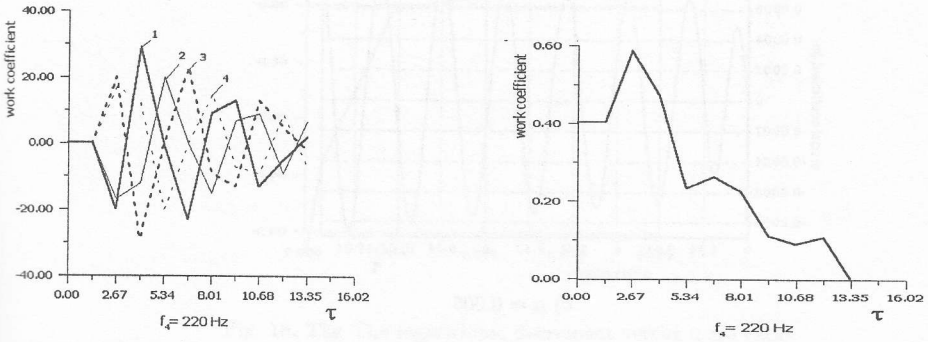

a) b)

Fig. 16. The coupled oscillations according to the 4^{th} mode, IBPA= +90 deg, $\delta = 0.195$, $t = \tau/316$ s.

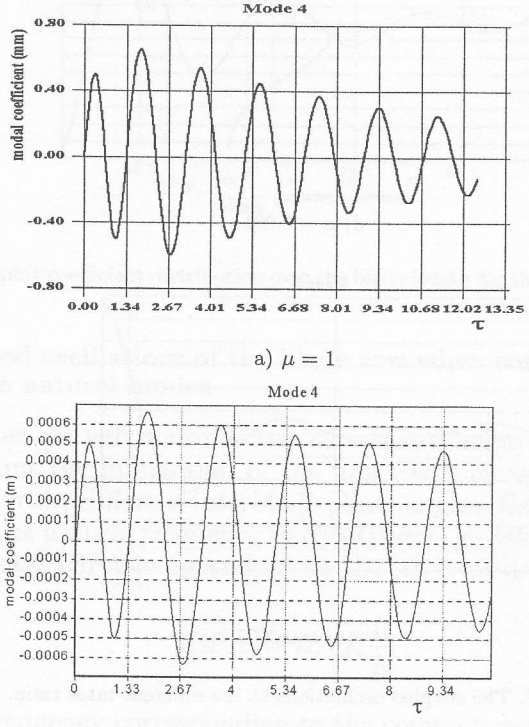

a) $\mu = 1$

b) $\mu = 0.01$

Fig. 17. The coupled oscillations at the different mass ratio.

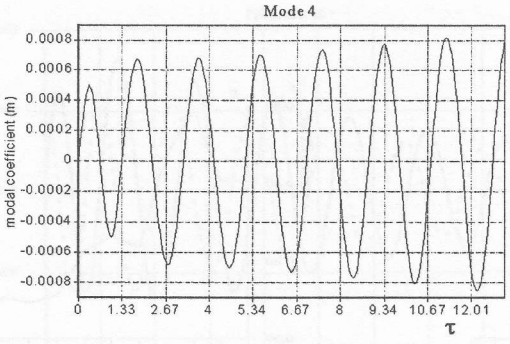

c) $\mu = 0.005$

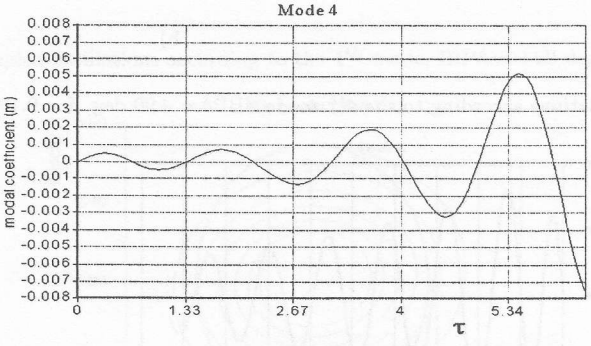

d) $\mu = 0.001$

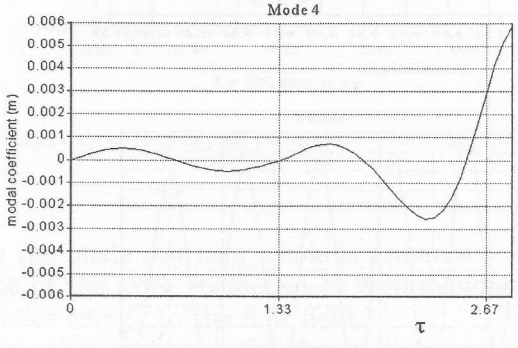

e) $\mu = 0.0001$

Fig. 17. The coupled oscillations at the different mass ratio.

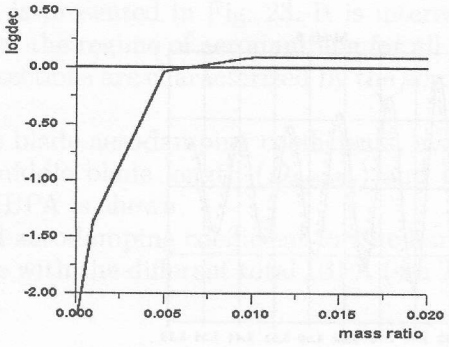

Fig. 18. The The logarithmic decrement versus mass ratio.

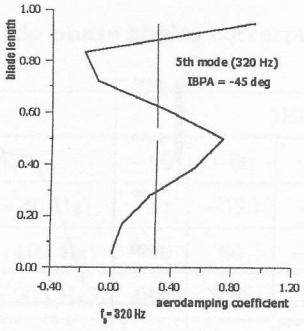

Fig. 19. The aerodamping coefficient distribution over the blade length for the 5^{th} mode, IBPA=-45 deg.

4.2. The coupled oscillations of the blade row when considering the interaction of five natural modes

In this chapter we will consider the aeroelastic behaviour of the blade row taking into account the interaction of the first five natural modes. Calculations were performed for the different interblade phase angles. Each of natural modes is characterized by its natural frequency of oscillations, so taking into consideration five modes, the total IBPA is dependant on the ith interblade phase angle $\mathrm{IBPA_i}$

$$\mathrm{IBPA}_i = \mathrm{IBPA}\frac{f_i}{f_0},$$

where f_0 is the frequency corresponding to the common period of oscillations (in our case 20 [Hz]), f_i the natural frequency for i-th mode. Tab. 1 shows the values of total IBPA corresponding to ith interblade phase angles.

The energy exchange between the gas flow and vibrating blades at the harmonic oscillations is characterized by value and sign of the aerodamping coefficient. The aerodamping coefficient distribution over the blade length for the total IBPA

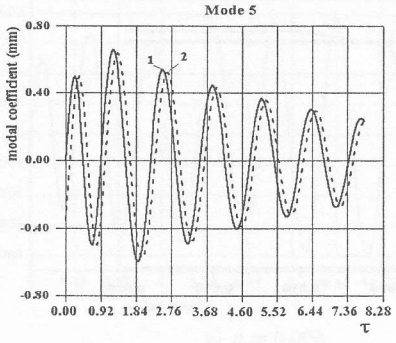

Fig. 20. The blade displacements at the coupled oscillations according to the 5^{th} mode, IBPA= -45 deg, $t = \tau/316$ s.

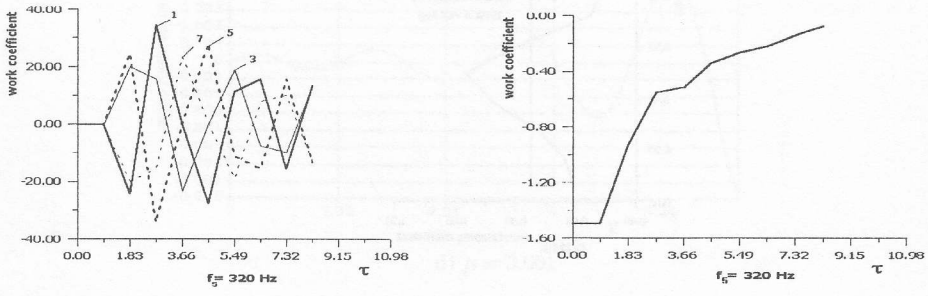

a) b)

Fig. 21. The work coefficient change at the coupled oscillations according to the 5^{th} mode, IBPA=-45 deg, $t = \tau/316$ s.

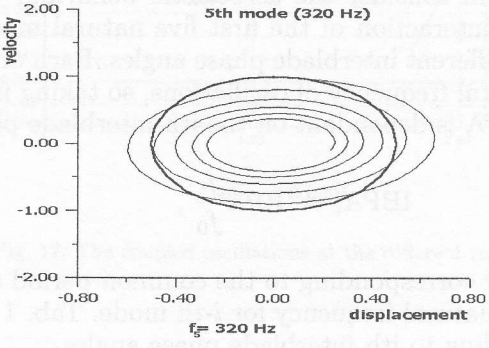

Fig. 22. The phase trajectory at the coupled oscillations according to the 5^{th} mode, IBPA=-45 deg.

shown in Tab. 1, is presented in Fig. 23. It is interesting to see that the middle blade sections is at the regime of aerodamping for all total IBPA values, while the peripheral blade sections are characterized by the aerodamping or the self-exciting vibration.

In Fig. 24 the blade aerodamping coefficients, averaged over the blade length (D_{aver}), in the middle blade length (D_{middle}) and the tip blade section (D_{per}) versus the total IBPA is shown.

The averaged aerodamping coefficient for the harmonic oscillations according to first five modes with the different total IBPA (see Tab. 1) is positive (damping) (see Figs. 23-24).

Table 1

The interblade phase angles corresponding to 5 natural modes

	IBPA, deg				
$IBPA_i$	−90	−60	−26	+45	+160
$IBPA_1$ ($f_1 = 40$ Hz)	180	−120	−50	90	−40
$IBPA_2$ ($f_2 = 100$ Hz)	−90	60	−130	−135	80
$IBPA_3$ ($f_3 = 200$ Hz)	180	120	105	90	160
$IBPA_4$ ($f_4 = 220$ Hz)	90	60	80	135	−40
$IBPA_5$ ($f_5 = 40$ Hz)	0	120	−50	0	40

The blade response is shown in Figs. 25-29. In Figs. 25 the aeroelastic blade behaviour of each of the natural modes separately can be seen. During the time interval from 0 to 14.64 s the harmonic oscillations take place, then after removing the kinematic excitation the coupled fluid-structure vibration continues. In this case the oscillations are damped. In Figs. 26-28 the response of the blade according to the 1-5 modes for different interblade phase angle is shown. Generally, in the case of considered blade the interblade phase angle does not change the response.

The logarithmic decrement of the coupled vibration for each modes as a function of the total IBPA is shown in Fig. 30.

The blade response for each of the natural modes is damped with the logarithmic decrement, which does not practically depend on the total IBPA value.

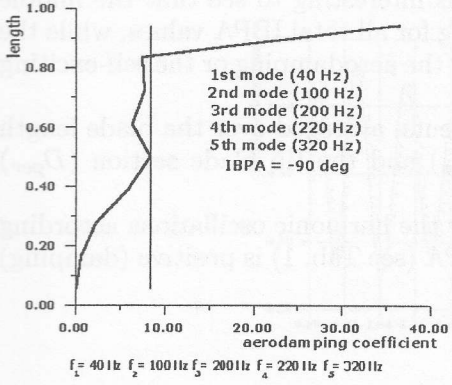

a)

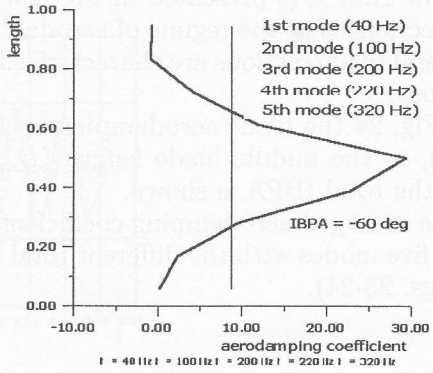

b)

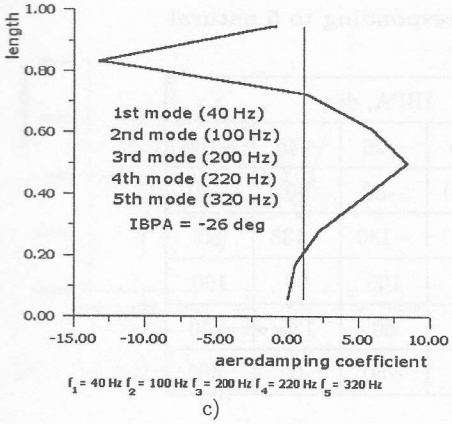

c)

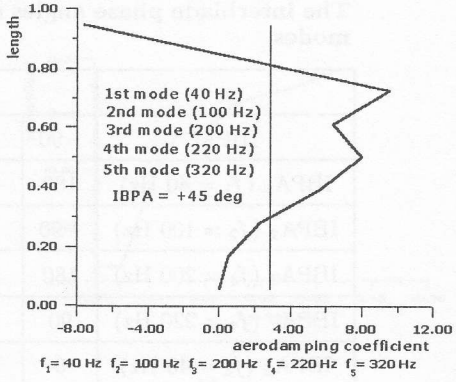

d)

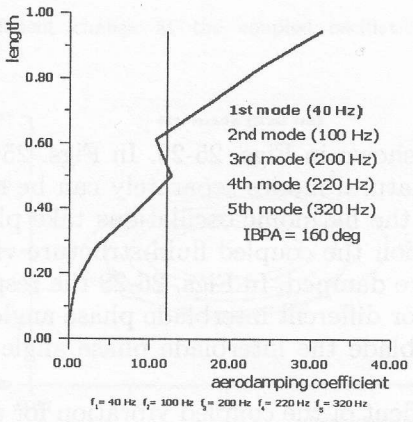

e)

Fig. 23. The aerodamping coefficient distribution over the blade length for the first 5 modes.

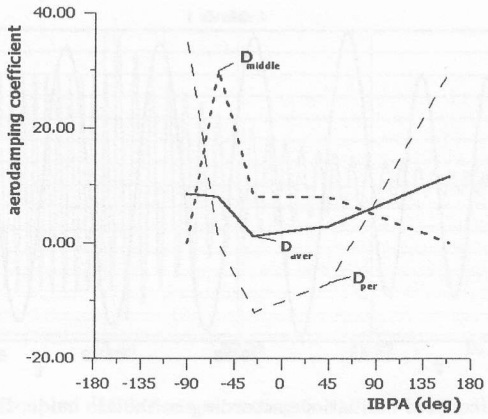

Fig. 24. The aerodamping coefficient versus the total IBPA.

5. Conclusions

In the present study, the simultaneous time domain method and the modal superposition method have been used to determine the aeroelastic stability of the cascade.

It is shown that the blade response for all considered regimes is damped.

The interaction between the natural modes leads to the practical independence of damping for each mode from IBPA value.

The interaction between the natural modes leads to different distribution of the aerodamping coefficient along the blade length in comparison to distribution for the particular mode shapes.

The sign of the aerodynamic coefficient may be considered only as a necessary but not sufficient condition for the existence of self-excited vibrations. The blade response depends on the energy value transfer from the flow to the blade, and on the blade kinetic energy at the coupled fluid- structure oscillations.

The calculation of the damping coefficient is very important from the forced vibration point of view, because generally blades are design out of resonance.

Acknowledegments The authors wishe to acknowledge KBN for the financial suport of this work (project 7 T07B 010 16). All numerical calculations were made at the Academic Computer Center TASK (Gdańsk, Poland)

Received 20 October 2000

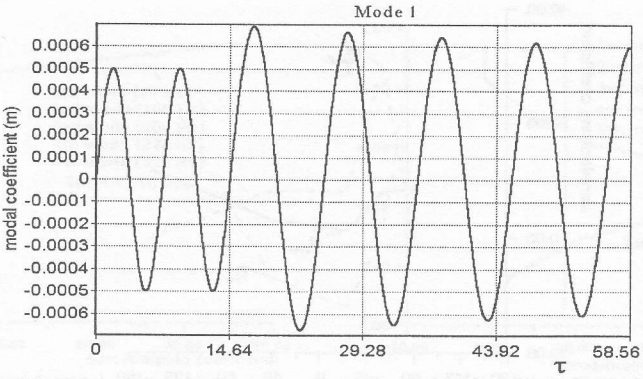

Fig. 25a. The coupled oscillations according to the 1^{st} mode, IBPA=−90 deg.

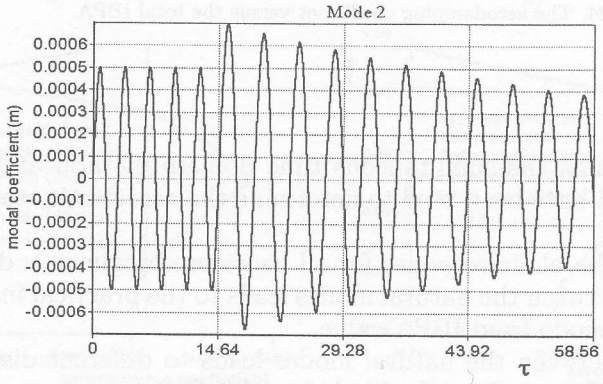

Fig. 25b. The coupled oscillations according to the 2^{nd} mode, IBPA=−90 deg.

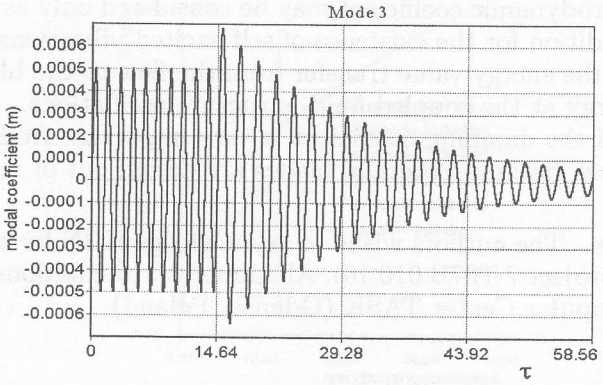

Fig. 25c. The coupled oscillations according to the 3^{rd} mode, IBPA=−90 deg.

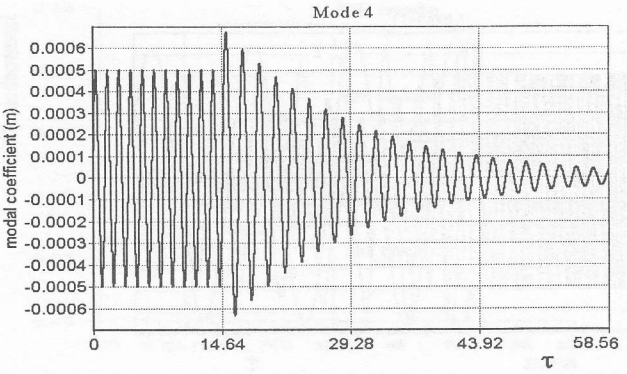

Fig. 25d. The coupled oscillations according to the 4^{th} mode, IBPA=−90 deg.

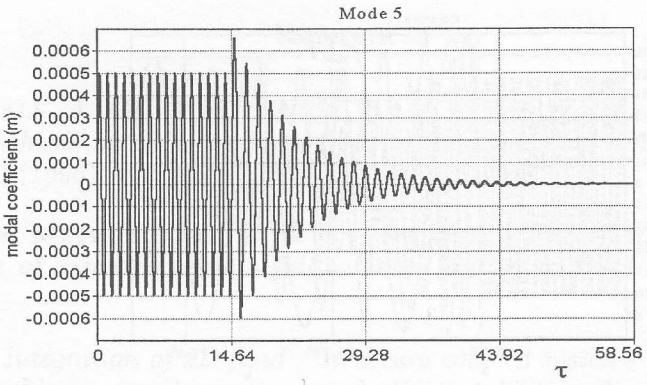

Fig. 25e. The coupled oscillations according to the 5^{th} mode, IBPA=−90 deg.

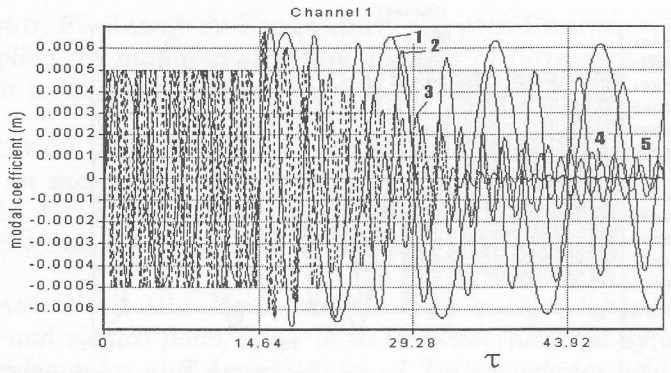

Fig. 26. The coupled oscillations according to the 1-5 modes, IBPA=−60 deg.

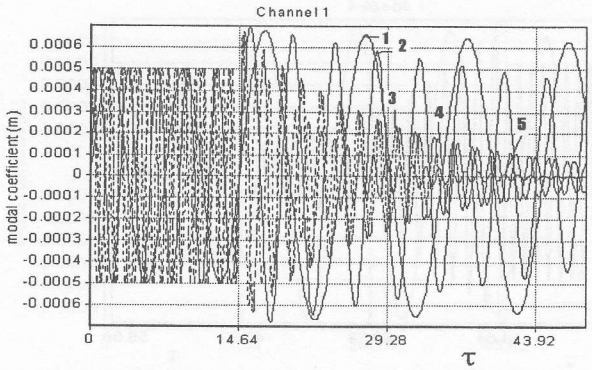

Fig. 27. The coupled oscillations according to the 1-5 modes, IBPA=−26 deg.

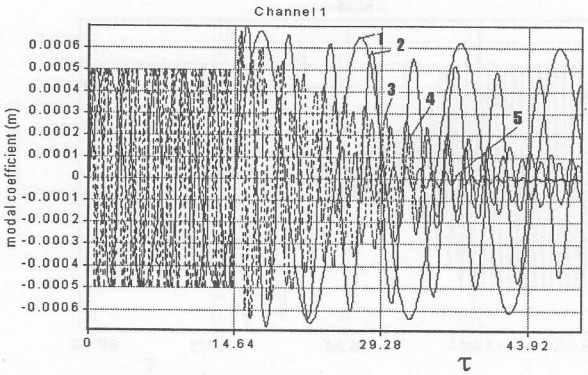

Fig. 28. The coupled oscillations according to the 1-5 modes, IBPA=+45 deg.

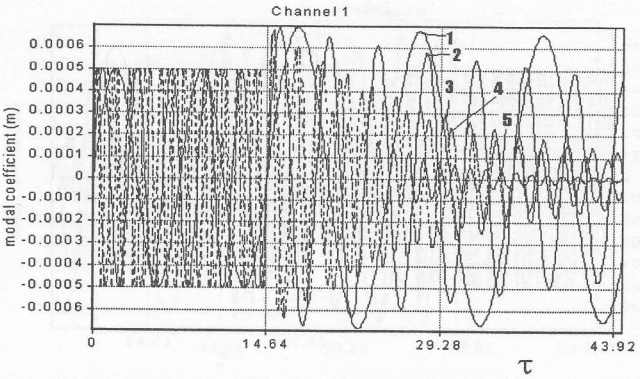

Fig. 29. The coupled oscillations according to the 1-5 modes, IBPA=+160 deg.

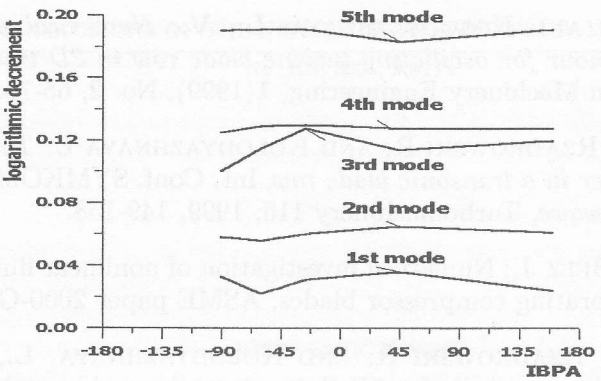

Fig. 30. The logarithmic decrement versus the interblade phase angle.

References

[1] MARSHALL, J. G. AND IMREGUN M.: *A Review of aeroelasticity methods with emphasis on turbomachinery applications*, Journal of Fluids and Structures, **10**(1996), 237-257.

[2] BAKHLE, M. A., REDDY, T. S. R., AND KEITH T.G.: *Time domain flutter analysis of cascades using a full-potential solver*, AIAA J. **30**(1992), No 1, 163.

[3] HE L.: *Integration of 2D fluid / structure coupled systems for calculation of turbomachinery aerodynamic, aeroelastic instabilities*, J. of Computational Fluid Dynamics, **3**(1984), 217.

[4] MOYROUD, F., JACQUET-RICHARDET, G., AND FRANSSON, T., H.: *A modal coupling for fluid and structure analysis of turbomachines flutter application to a fan stage*, ASME Paper 96-GT-335, 1-19.

[5] RZĄDKOWSKI, R., GNESIN, V. AND KOVALOV, A.: *The 2D flutter of bladed disc in an incompressible flow*, Proc. of the 8th International Symposium *Unsteady Aerodynamics and Aeroelasticity of Turbomachines* held in Stockholm, Sweden, Sept. 14-18.1998, 317-334.

[6] HE L. AND NING W.: *Nonlinear harmonic analysis of unsteady transonic inviscid and viscous flows*, Proc. of the 8th International Symposium *Unsteady Aerodynamics and Aeroelasticity of Turbomachines* held in Stockholm, Sweden, Sept. 14-18.1998, 183-189.

[7] BENDIKSEN, O.: *Nonlinear blade vibration and flutter in transonic rotors*, Proc. of ISROMAC-7, 7th Int. Symp. on *Transport Phenomena and Dynamics of Rotating Machinery*, Feb., 22-26.1998, Honolulu, Hawaii, USA, 664.

[8] Gnesin, V., I., and Kolodyazhnaya, L., V.: *Numerical modelling of aeroelastic behaviour for oscillating turbine blade row in 3D transonic ideal flow*, Problems in Machinery Engineering, **1**(1999), No. 2, 65-76.

[9] Gnesin, V., I., Rządkowski R. and Kolodyazhnaya L: *The numerical study of 3D flutter in a transonic blade row*, Int. Conf. SYMKOM'99 *Cieplne Maszyny Przepywowe*, Turbomachinery 115, 1999, 149-158.

[10] Carstens V., Belz J.: Numerical investigation of nonlinear fluid-structure interaction in vibrating compressor blades, ASME paper 2000-GT-0381.

[11] Gnesin, V., I., Rządkowski R. and Kolodyazhnaya, L., V.: *A coupled fluid-structure analysis for 3D flutter in turbomachines*, ASME paper 2000-GT-0380.

[12] Gnesin V.,I., Rządkowski R.: *The theoretical model of 3D flutter in subsonic, transonic and supersonic inviscid flow*, Transaction of Institute of Fluid-Flow Machinery, **106**(2000), 45-68.

[13] Godunov, S., K. et al.: *Numerical solution of multidimensional problems in gasdynamics*, Nauka, M., 1996, (in Russian).

[14] Rządkowski, R.: *Dynamics of steam turbine blading. Part two: Bladed discs*, Ossolineum, Wrocaw-Warszawa 1998.

[15] Rządkowski, R., Gnesin, V: *The numerical and experimantal verification of the 3D inviscid code*, Transaction of Institute of Fluid-Flow Machinery, **106**(2000), 69-95.

[16] Rządkowski R., Gnesin V.: *Aeroelastic behaviour of the last stage steam turbine blades row. Part I. Harmonic oscillations*, Transaction of Institute of Fluid-Flow Machinery, **22**(2001), No. 1-2, 59-72.